Physica E 44 (2012) 981–984

Contents lists available at ScienceDirect

Physica E

journal homepage: www.elsevier.com/locate/physe

Quantum transport modeling of defected graphene nanoribbons

I. Deretzis [a,b,*], G. Fiori [c], G. Iannaccone [c], G. Piccitto [d], A. La Magna [b]

[a] Scuola Superiore, Universitá di Catania, Via San Nullo 5/i, 95123 Catania, Italy
[b] Istituto per la Microelettronica e Microsistemi (CNR-IMM), Z.I. VIII Strada 5, 95121 Catania, Italy
[c] Dipartimento di Ingegneria dell'Informazione: Elettronica, Informatica, Telecomunicazioni, Via Caruso 16, 56122 Pisa, Italy
[d] Dipartimento di Fisica e Astronomia, Universitá di Catania, Via Santa Sofia 64, 95123 Catania, Italy

ARTICLE INFO

Article history:
Received 19 May 2010
Received in revised form
15 June 2010
Accepted 18 June 2010
Available online 23 June 2010

ABSTRACT

We study backscattering phenomena during conduction for graphene nanoribbons of μm lengths, from single vacancy scatterers up to finite defect concentrations. Using *ab initio* calibrated Hamiltonian models we highlight the importance of confinement and geometry on the shaping of the local density of states around the defects that can lead to important alterations on the transport process, giving rise to impuritylike conduction gaps in the conductance distribution. Within a statistical analysis of finite defect concentration we show that conductance degradation can become very important.

1. Introduction

Graphene is a semimetallic two-dimensional electron gas system that has gained important attention due to its peculiar electrical, mechanical and optical characteristics [1]. When confined in one dimension graphene can also obtain a bandgap that makes it an ideal candidate for post-Si CMOS integration. However, the presence of topological defects (e.g. vacancies, impurities) gives rise to resonant quasibound states [2] that can significantly alter the transport characteristics by inducing conduction gap features in the proximity of the charge neutrality point [3–6]. At the same time high concentrations of defects can strongly downgrade electron mobilities [7]. Under this perspective a thorough investigation of the scattering mechanism in graphene nanoribbons becomes crucial for the device potential of these systems.

In this article we attempt a bottom up approach in the study of electron backscattering phenomena for vacancy-damaged graphene nanoribbons that ranges from the physical effect of the single scatterer in the nanoscale up to a statistical analysis of finite defect concentration for ribbons with μm lengths. To this end we use accurately parameterized semiempirical Hamiltonians from first principles that account for the bandstructure of sp^2-hybridized carbon as well as the correct energy resonance of the defect states. Results show that there is a clear relationship between the position of the vacancy, the resonance of the defect states, and the local density of states of the corresponding unperturbed system. Coupling between such features can give rise to backscattering effects during the conduction process that in the case of the first $\pi-\pi^*$ plateau are associated with the opening of conduction pseudogaps. In the statistical limit of finite defect concentrations we show that conductance downgrading can be very large throughout the energy spectrum, compromising graphene's typical transport characteristics.

2. Methodology

Armchair and zigzag graphene nanoribbons (AGNRs and ZGNRs respectively) are classified using the convention of Ref. [8], i.e. with the integer N_a (N_z) indicating the number of dimer lines (zigzag chains) across the ribbon width. We use two *ab initio* parameterized semiempirical Hamiltonians with different levels of accuracy for the correct treatment of defect states in the sp^2-hybridization scheme. The first one is formed on the basis of the extended Hückel theory, using a double-ζ sp^3d^5 Slater orbital basis set [9]. Such Hamiltonian accounts for next-to-near neighbor interactions in a natural way and accurately assigns the resonance of the vacancy states [4]. The second one is the nearest-neighbor tight-binding Hamiltonian with a $t_0=2.7$ eV hopping parameter, whereas on-site energies and hopping integrals for the defected sites have been appositively parameterized in order to reproduce first-principles and extended Hückel results [10]. Quantum transport is studied within the non-equilibrium Green's function (NEGF) formalism coupled to the Landauer–Buttiker approach [11] for the calculation of the conductance g. A two-terminal geometry is considered throughout the article where the defected region corresponds to the active device part. Contacts are ideal, i.e. of the same width N_a (N_z)

* Corresponding author at: Istituto per la Microelettronica e Microsistemi (CNR-IMM), Z.I. VIII Strada 5, 95121 Catania, Italy. Tel.: +39 095 5968321; fax: +39 095 5968312.
E-mail address: ioannis.deretzis@imm.cnr.it (I. Deretzis).

1386-9477/$ - see front matter © 2010 Elsevier B.V. All rights reserved.
doi:10.1016/j.physe.2010.06.024

as the device without the presence of vacancies. Edges are passivated with hydrogen (directly for the extended Hückel Hamiltonian and following the *ab initio* calibration of Ref. [8] in the tight-binding case).

3. Backscattering by single vacancies

We start by identifying backscattering effects due to the presence of single vacancies in various types of GNRs. In all cases the response of the defect is to give rise to quasilocalized states [12] along non-localized ones, that due to electron–hole disparity do not preserve a mirror symmetry with respect to the Fermi level of the system. The repercussions of quasibound states on the conductance are not uniform, but depend on purely geometrical criteria, giving rise to two distinct transport behaviors. Fig. 1a,b shows conductance spectra for a semimetallic 35-AGNR where a single vacancy has been introduced in two neighboring positions of a chain transversal to the longitudinal axis of the systems. In the first case significant conductance dips and pseudogap features are present within the valence band of the first $\pi-\pi^*$ plateau of the system. In the second case the pure structure's first conductance plateau remains unaltered. A systematic study for all dimer line positions N_a (that is valid for all semimetallic AGNRs in this study) shows that two-thirds of the total sites belong to the first group, while the remaining one-third conforms with the second group, according to the following rule: for $N_a=3p+2$ dimer lines ($\forall p \in \mathbb{N}$), vacancies at the $N_a=3q$ sites do not affect the first conductance plateau ($\forall q \in \mathbb{N}, \leq p$), while the rest give rise to conductance pseudogaps at energies lower than the charge neutrality point. The resonance of these pseudogaps is related to the resonance of the defect states within this plateau under the description of an electronic Hamiltonian that breaks electron–hole symmetry[1] [4] and have strong similarities with backscattering effects obtained by p-type impurities [13]. In a similar manner, defected semiconducting AGNRs have preferential sites that give conductance dips in addition to the intrinsic bandgap, without however generally satisfying the previous rule (see Fig. 1c,d). The case of ZGNRs is even more particular since vacancy positioning can influence regions both above and below the charge neutrality point. In this sense vacancies in ZGNRs become similar to impurities with both donor and acceptor characteristics (Fig. 1e,f). Likewise to AGNRs, not all available sites give rise to this behavior and there are also important alterations of the conduction gap resonances with respect to the vacancy position.

The fundamental characteristic of the previously presented picture, i.e. the manifestation of pseudogap features in the first conductance plateau of defected graphene nanoribbons, has an important geometrical aspect: the ribbon's confinement and the positioning of the vacancy site become crucial for the presence or not of conductance dips. The origin of such mechanism lies in localized or expanded perturbations of the density of states of the systems in study in the presence of topological defects. It is well known that one-dimensional confinement plays a particular role in the shaping of GNR wavefunctions, giving rise to local alterations of the wavevector's value [4]. When a defect's location coincides with a zero (or extremely small) wavevector value for a given GNR, the perturbation induced on the electronic structure remains spatially and energetically local. Contrary, when the

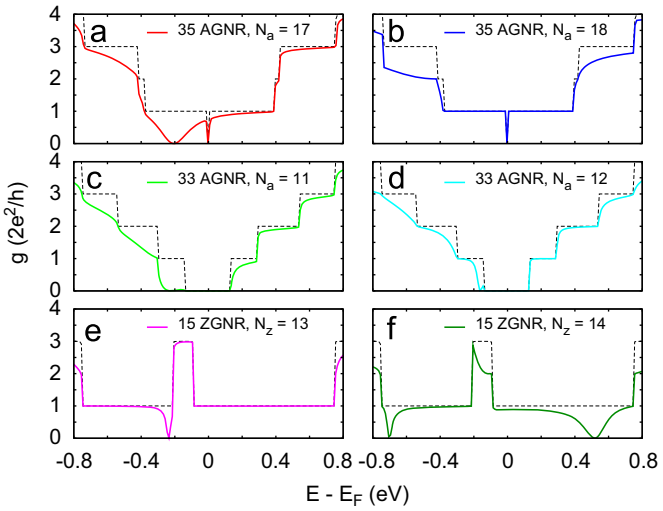

Fig. 1. Conductance distribution g as a function of energy for (a) a 35-AGNR with a single vacancy at $N_a=17$, (b) a 35-AGNR with a single vacancy at $N_a=18$, (c) a 33-AGNR with a single vacancy at $N_a=11$, (d) a 33-AGNR with a single vacancy at $N_a=12$, (e) a 15-ZGNR with a single vacancy at $N_z=13$, (f) a 15-ZGNR with a single vacancy at $N_z=14$.

defect lies in a GNR region with a finite wavevector value such perturbation expands both spatially and energetically [4]. The sum of perturbative behaviors due to the quasilocalized defect states within the first conductance plataeu give rise to an increased DOS distribution with respect to the ideal case. This expanded perturbation is the reason for electron backscattering during conduction. This concept can be visualized better through local density of states distributions LDOS($\vec{r}$,E) at the positions $\vec{r}$ of the device atoms at energy E:

$$LDOS(\vec{r},E)=\sum_{\alpha}|\Psi_{\alpha}(\vec{r})|^2\delta(E-\varepsilon_{\alpha}), \quad (1)$$

where ε_{α} are energy eigenstates, Ψ_{α} their respective eigenfunctions and δ is the Delta function, while summing over all atoms gives the total DOS of the system at energy E. In the case of a system with semi-infinite contacts the LDOS can be calculated within the NEGF. Fig. 2a–c shows LDOS values for different energies within the first plateau for a 38-aGNR with a vacancy at $N_a=19$. It is clear that a perturbation around the vacancy site spreads over the entire range of energies that corresponds to the conductance dip. Contrary, for $N_a=18$ no extended perturbation can be detected (see Fig. 2d). The mechanism is similar also for the other types of GNRs, respecting however the different form of the wavevectors within the first conductance plateau. According to the particular system, defects can provoke expanded or localized perturbations of the LDOS in different parts of the energy spectrum that give rise to backscattering effects.

4. Statistical conductance analysis for finite defect distributions

Understanding of single-vacancy scattering forms the basis of the generalized backscattering mechanism present in confined graphene systems. However transport repercussions for realistic devices within the micro-scale and a finite concentration of defects can only be addressed within statistical analyses of large replicas of equivalent systems. For this purpose we have appositively calibrated a next-neighbor TB Hamiltonian that reproduces results obtained by more accurate Hamiltonians in the case of single vacancies [3,10]. Fig. 3 shows statistical

[1] Simple first-neighbor tight-binding Hamiltonians preserve an electron–hole symmetry in the description of the electronic structure of GNRs. In the case where vacancies are introduced in the formalism by zeroing hoppings from and to the defected site, the resonance of the defect state falls at zero energy. Such description is revised by further-neighbor electronic Hamiltonians [4,10].

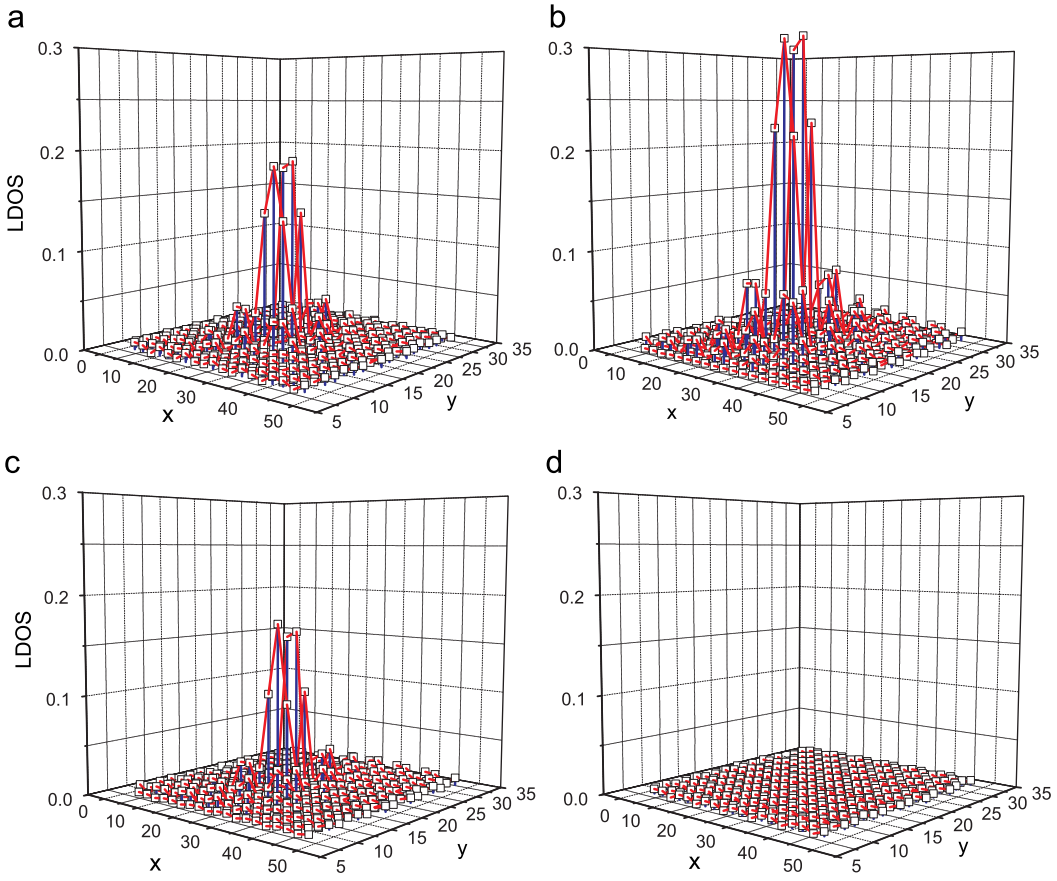

Fig. 2. LDOS as a function of distance coordinates (in Å) and energy (in eV) for a defected 38-AGNR. Defect position N_a and energy E are at (a) $N_a=19$, $E=0.27$ eV, (b) $N_a=19$, $E=0.17$ eV, (c) $N_a=19$, $E=0.07$ eV, and (d) $N_a=18$, $E=0.17$ eV. The zero energy level refers to the charge neutrality point.

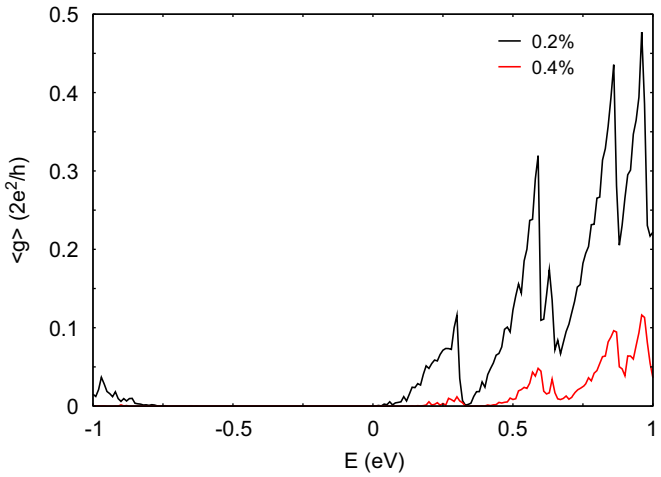

Fig. 3. Average conductance $\langle g \rangle$ as a function of the energy E, for a vacancy damaged 47 AGNR. Plotted values represent statistical averages over more than 500 equivalent replicas of the system. Charge neutrality points of pure and defected systems are aligned at $E=0$ in the figure.

averages for the conductance of a 0.84 μm long 47 AGNR with two finite defect concentrations (0.2% and 0.4% respectively), obtained for more than 500 equivalent replicas of these systems. Like in the single vacancy case, a pseudogap appears in the hole-band region close to the Fermi level of the system. By means of a scaling analysis [14,15] we found that the conduction regime varies with the energy of the charge carriers, passing from the localization regime (the localization length ξ is $\sim$40 nm in the center of the conduction gap for the 0.2% case) to the quasi-diffusive one away from the conduction gap (the elastic mean free path l_e is $\sim$0.4 μm when $E\sim1$ eV for the 0.2% case). However, the main issue arising from multiple scatterers is the significant downgrading of the conductance throughout the energy spectrum that increases with the defect concentration. It is also evident that for heavily damaged GNRs (defect concentrations of 0.4% here) conductance becomes extremely low and typical graphene-like properties practically vanish. Crystalline quality is therefore a fundamental prerequisite for the maintenance of device-related characteristics like high electron mobilities and current densities.

5. Discussion

In this article we have examined the role of vacancy defects in the conduction mechanism of graphene nanoribbons, from single scatterers to finite concentrations in μm- sized GNRs. Results have shown that vacancies can give rise to impurity-like pseudogaps in the first conductance plateau of these systems on the basis of purely geometrical criteria. The underlying mechanism is subject to localized or expanded perturbations of the density of states of these systems according to the positioning of the defect and the confinement of the GNR. Large-scale statistical analyses have shown that a finite defect concentration can significantly downgrade the conducting capacity of these systems with important repercussions in the entire conductance distribution. Based on this picture particular attention should be paid for the presence of

defects in GNR samples since the backscattering mechanism can on one hand allow for the engineering of mobility gaps while on the other it can negatively affect important conduction properties like electron mobility and high carrier density.

It is expected that a more realistic description of quantum transport in defected GNRs should also account for the presence of non-ideal contacts, introducing in the computational formalism elements that deal with the chemical bonding between the GNR and the metallic lead as well as electrostatic aspects like the presence of Schottky barriers due to work function differences [16]. In this sense we can expect new features arising with a chemical/electrostatic background that should act complementary or even interact with the scattering effects presented in this paper. A thorough investigation towards this direction would allow for a more concrete understanding of the quantum transport process in these systems.

Acknowledgements

This work has been partially supported by the European Science Foundation (ESF) under the EUROCORES Programme EuroGRAPHENE CRP GRAPHIC-RF.

References

[1] A.H.C. Neto, F. Guinea, N.M.R. Peres, K.S. Novoselov, A.K. Geim, Reviews of Modern Physics 81 (1) (2009) 109.
[2] H.J. Choi, J. Ihm, S.G. Louie, M.L. Cohen, Physical Review Letters 84 (2000) 2917.
[3] A. La Magna, I. Deretzis, G. Forte, R. Pucci, Physical Review B 80 (19) (2009) 195413.
[4] I. Deretzis, G. Fiori, G. Iannaccone, A. La Magna, Physical Review B 81 (8) (2010) 085427.
[5] B. Biel, F. Triozon, X. Blase, S. Roche, Nano Letters 9 (2009) 2725.
[6] S.M.M. Dubois, A. Lopez-Bezanilla, A. Cresti, F. Triozon, B. Biel, J.-C. Charlier, S. Roche, ACS Nano 4 (4) (2010) 1971.
[7] J. Chen, W.G. Cullen, C. Jang, M.S. Fuhrer, E.D. Williams, Physical Review Letters 102 (23) (2009) 236805.
[8] Y. Son, M.L. Cohen, S.G. Louie, Physical Review Letters 97 (21) (2006) 216803.
[9] D. Kienle, J.I. Cerda, A.W. Ghosh, Journal of Applied Physics 100 (4) (2006) 043714.
[10] I. Deretzis, G. Forte, A. Grassi, A. La Magna, G. Piccitto, R. Pucci, Journal of Physics Condensed Matter 22 (9) (2010) 095504.
[11] S. Datta, in: H. Ahmed, M. Pepper, A. Broers (Eds.), Electronic Transport in Mesoscopic Systems, Cambridge University Press, Cambridge, 1995.
[12] V.M. Pereira, J.M.B. Lopes Dos Santos, A.H. Castro Neto, Physical Review B 77 (11) (2008) 115109.
[13] B. Biel, X. Blase, F. Triozon, S. Roche, Physical Review Letters 102 (9) (2009) 096803.
[14] A. Cresti, S. Roche, Physical Review B 79 (23) (2009) 233404.
[15] A. La Magna, I. Deretzis, G. Forte, R. Pucci, Physical Review B 78 (15) (2008) 153405.
[16] I. Deretzis, G. Fiori, G. Iannaccone, A. La Magna, work in progress.